J. Fluid Mech. (2005), *vol.* 543, *pp.* 45–55.
doi:10.1017/S0022112005006786 Printed in the United Kingdom

The timing of vortex shedding in a cylinder wake imposed by periodic inflow perturbations

By E. KONSTANTINIDIS†, S. BALABANI AND M. YIANNESKIS

Experimental and Computational Laboratory for the Analysis of Turbulence, Department of Mechanical Engineering, King's College London, Strand, London WC2R 2LS, UK

(Received 11 May 2005 and in revised form 17 August 2005)

The interaction of vortex shedding from a circular cylinder with an inflow which has low-amplitude periodic velocity oscillations (perturbations) superimposed upon it, was investigated experimentally by means of particle image velocimetry. The experiments were made at three perturbation frequencies across the lock-on range in which the vortex shedding frequency is synchronized with the subharmonic of the imposed frequency. The basic wake pattern in this range is antisymmetric vortex shedding, i.e. the familiar 2S mode. The timing of vortex shedding is defined with respect to the cross-flow oscillation of the wake which is found to play a critical role. Quantitative analysis of the phase-referenced patterns of vorticity distribution in the wake shows that a vortex is actually shed from the cylinder when the cross-flow oscillation of the wake is strongest, marked by a sudden drop in the computed vortex strength. At the middle of the lock-on range, shedding occurs near the minimum inflow velocity in the cycle or, equivalently, during the forward stroke of a cylinder oscillating in-line with the flow. It is argued that the imposed timing of vortex shedding relative to the cylinder motion induces a negative excitation from the fluid, which might explain why the in-line response of a freely vibrating cylinder exhibits two positive excitation regions separated by the lock-on region found in forced oscillations.

1. Introduction

Over the past few decades the study of so-called 'bluff' body wakes, and in particular that of the circular cylinder, has been driven by an urge to understand vortex-induced vibration, which is of concern in the design of many engineering structures. The fundamental research in the field has proceeded using two complementary approaches: some investigators consider the problem where a rigid cylinder is forced to oscillate in a predefined direction simulating the vortex-induced motion, while others consider the case where the cylinder is flexibly mounted at the ends and free to vibrate with a single and, more recently, with two degrees of freedom. Both transverse to the flow and streamwise oscillations have been considered in numerous studies but the former case has attracted most of the interest. Recently, Carberry *et al.* (2004) explored the relationship between free and forced transverse oscillations of a rigid cylinder. A strong similarity was observed between the response branches of the freely oscillating cylinder and the wake modes of the forced cylinder in terms of the patterns of vorticity

† Present address: Department of Engineering and Management of Energy Resources, University of Western Macedonia, Kozani 50100, Greece.

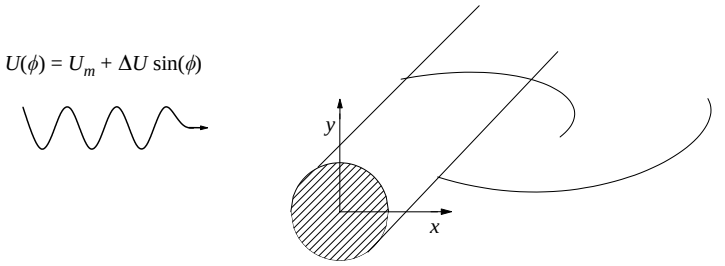

FIGURE 1. Schematic description of the flow configuration.

and the variation of the phase of the total and vortex lift forces with respect to the cylinder motion. Central to their analysis is the decomposition of the total lift force into two components: the apparent mass force due to acceleration of the cylinder and the vortex lift force due to the vorticity distribution in the wake. It turns out that the phase of the vortex lift force determines the phase of the total force which, in turn, determines whether the energy transfer is from the fluid to the cylinder or vice versa.

In contrast, the understanding gained from studies of cylinders oscillating in-line with the flow, either freely or forcibly, has remained largely unexplored although a considerable amount of force data exists in the published literature. What appears to be missing is the phase-referenced patterns of vorticity in the wake across the 'lock-on' range in which vortex shedding synchronizes with the cylinder oscillation. Only qualitative information from flow visualization studies can be found (Griffin & Ramberg 1976; Ongoren & Rockwell 1988). In this paper, we report on particle image velocimetry measurements obtained in the forced wake of a circular cylinder in an incident flow with low-amplitude periodic velocity oscillations (perturbations) superimposed upon it. This case is equivalent to that of a cylinder forced to oscillate in-line with a steady incident flow as long as the perturbation wavelength is large compared to the cylinder diameter, a condition which is satisfied in the present experiments. An attempt is made to identify the underlying mechanics of wake excitation across the synchronization range in terms of the patterns and the timing of the vortex shedding process. In the light of the present findings, some aspects of the in-line free-vibration response of a circular cylinder are discussed in the paper. It is hoped that this study will complement other contributions dealing with bluff-body wakes, in particular those concerned with bodies in unsteady flows, and will improve understanding of vortex-induced vibrations for this class of flows.

2. Experimental system and conditions

A brief description of the experimental facility and measurement techniques is given below. For further details, the reader may refer to previous publications by the authors (Konstantinidis, Balabani & Yianneskis 2003, 2004, 2005). A schematic description of the flow configuration is shown in figure 1. The experiments were carried out in a recirculating-type water tunnel having a 72 mm-square cross-section. A circular rod of diameter $D = 7.2$ mm was centrally mounted in the test section. The incident flow was made uniform by a contraction (area ratio 9:1) which preceded the test section and had a background turbulence level of 3.3 %. Periodic velocity oscillations were superimposed onto the mean incident flow via the action of a rotating valve. Flow conditions were monitored by laser-Doppler velocimetry (LDV) measurements upstream of the test cylinder. The inflow velocity can be approximated

U_m (m s^{-1})	f_e (Hz)	ΔU (m s^{-1})	Re	f_e/f_o	A/D
0.301	15.4	0.019	2170	1.74	0.053
0.299	17.1	0.018	2160	2.00	0.044
0.298	19.5	0.018	2150	2.20	0.042

TABLE 1. Flow parameters employed in the experiments.

as a function of the phase-angle ϕ by $U(\phi) = U_m + \Delta U \sin(\phi)$; U_m is the mean inflow velocity and ΔU is the amplitude of velocity oscillation. The phase-angle ϕ relates to 'virtual' time t via $\phi = 2\pi f_e t$ with f_e being the frequency of the imposed inflow perturbations. The independent parameters employed to describe the problem are: the Reynolds number $Re = U_m D/\nu$ (where ν is the kinematic viscosity of water), the frequency ratio, f_e/f_o, and the peak-to-peak amplitude of the equivalent cylinder oscillation $A/D = 2\Delta U/2\pi f_e D$. Herein, f_o is the natural vortex shedding frequency in unforced flow which was computed from a constant-Strouhal-number relationship $S = f_o D/U_m = 0.215$. The results reported in this paper were obtained for the conditions shown in table 1, i.e. at three perturbation frequencies with the mean inflow velocity and the amplitude of the velocity oscillations maintained nearly constant. The equivalent amplitude of cylinder oscillation A/D varies slightly with f_e/f_o. These conditions correspond to the primary lock-on (or synchronization) range for in-line cylinder or equivalent flow oscillations, in which the vortex shedding frequency locks on to the subharmonic of the imposed perturbation frequency (Konstantinidis *et al.* 2003).

The instantaneous velocity field of the near wake was examined using digital particle image velocimetry (DPIV). For this purpose the flow was seeded with 10 μm silvered micro-spheres and the wake was illuminated by a laser sheet perpendicular to the cylinder axis at midspan. Pairs of images were captured on a digital camera with a resolution of 1280×1024 pixels. The image pairs were analysed by employing adaptive cross-correlation on a 32×32-pixel interrogation window and a 50 % overlap ratio, giving a measurement-grid resolution of approximately $0.1D$. All images taken were phase-referenced with respect to the phase of the inflow oscillation. Phase information was provided by a high-precision optical encoder attached to the shaft of the perturbation-generating rotating valve. This enabled segregation of repetitive from non-repetitive incoherent flow structures by averaging at constant phase. The phase-averaged vorticity fields were calculated from thirty or more instantaneous fields.

3. Results

The instantaneous vorticity fields in the wake of the cylinder revealed two different vortex patterns which correspond loosely to the known 2S and 2P modes observed in transverse cylinder oscillations where two single and two pairs of vortices, respectively, are shed during each cycle of oscillation (Williamson & Roshko 1988). These patterns have also been observed in flow visualizations of a cylinder wake during in-line oscillations at $Re = 190$ by Griffin & Ramberg (1976). In the present study, the two patterns coexist at $f_e/f_o = 1.74$ whereas only the 2S mode was observed at $f_e/f_o \geqslant 2$. Examination of the instantaneous vorticity fields indicated that the interchange between the two modes was random and did not involve a change in the timing of vortex shedding with respect to the inflow oscillation. Previous analysis by means of proper orthogonal decomposition has shown that the most energetic wake mode has a 2S structure while the 2P pattern appears as a secondary effect (Konstantinidis

et al. 2004). In the following, the results only for the 2S mode are shown in order to facilitate direct comparisons at different frequencies. However, this does not limit the generality of the results since the wake characteristics discussed below were quite similar for both patterns.

The interaction between the inflow perturbations and the vortex shedding process in the wake is examined and an attempt is made to identify critical events which determine the timing of vortex shedding, i.e. the phase at which a vortex pinches off from the cylinder with respect to the inflow velocity oscillation. Descriptions of the mechanics of vortex formation and shedding in the unforced cylinder wake at subcritical Reynolds numbers can be found in Gerrard (1966) who has demonstrated the critical role of the flow oscillations across the wake axis and within the vortex formation region. This characteristic will prove useful also in the present context.

An obstacle in the study of wake flows is that it is difficult to find a consistent way to compute the circulation of the vortices, or vortex strength, especially when these are attached to the cylinder. To circumvent this problem, the following computational procedure was employed. Initially, individual vortices were identified in the phase-averaged vorticity fields $\langle\omega\rangle$ by the peaks in the absolute vorticity magnitude, denoted ω_p. The circulation around the peak locations was then computed by a closed-pathline integral for increasing radii and the maximum circulation was found; $r_{\max}$ is the corresponding radius. Generally, the behaviour observed was that the circulation initially increases, reaches a plateau and then drops off again with increasing radii. Subsequently, the vortex strength Γ and centroid $\{x_c, y_c\}$ were computed using surface integration (quadrature) of the vorticity distribution within the area enclosed by $r_{\max}$ as described, for example, in Cantwell & Coles (1983). The integration was performed only for values such that $\langle\omega\rangle \geqslant 0.15\omega_p$ in order to minimize the influence of noisy data. The above procedure enabled computation of the vortex strength in a well-defined and consistent way. Furthermore, the results provide physical insight into the shedding process as it is described below.

Figure 2 shows the vorticity distribution in the near wake at five phases during an imposed oscillation cycle (corresponding to half a vortex shedding cycle). In this figure, attention is directed to the clockwise-rotating (negative) vortex enclosed by the velocity vectors in subplots (*a–e*) and the corresponding variations in its strength along the wake, Γ, the imposed velocity oscillation, $U(\phi)$, and the velocity oscillation across the wake axis at the location in which its root-mean-square value is maximum, $V(\phi)$, in subplots (*f–h*), respectively. The tails of the velocity vectors shown delineate a circle which corresponds to the circular path of integration where the maximum circulation around the vortex was computed. However, the vortex strength estimates shown in figure 2(*f*) were computed from a quadrature as explained above. The following events occur in label sequence: (*a*) The vortex, fed with circulation from the cylinder, attains its maximum strength. At this phase, the inflow decelerates (equivalent to a cylinder moving forward in a steady inflow). (*b*) $V(\phi)$ is about to become strongest as the lower-side shear layer is entrained across the wake axis and cuts off the supply of vorticity when the inflow velocity attains its minimum value (cylinder moving forward at maximum speed). (*c*) The shed vortex picks up strength from the shear layer feeding in vorticity as the 'potential' flow outside the wake accelerates (cylinder at forwardmost position). (*d*) As the inflow velocity approaches its maximum value the vortex strength reaches a secondary maximum (cylinder in backward stroke). (*e*) The inflow starts to decelerate and the shed vortex moves downstream with gradually diminishing strength (cylinder towards its backwardmost position).

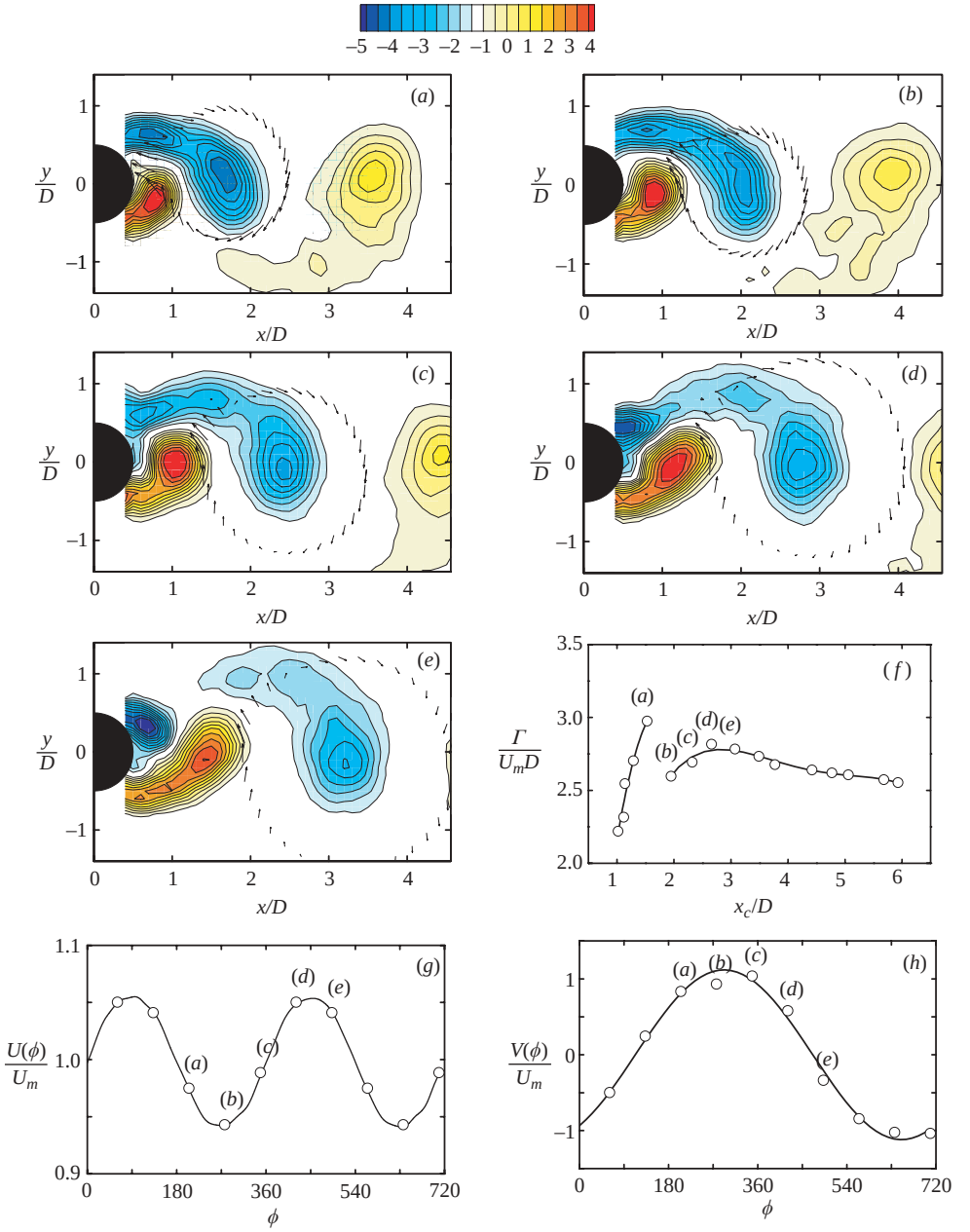

FIGURE 2. (*a–e*) Phase-averaged vorticity distributions in the wake showing the vortex shedding process at $f_e/f_o = 2$. Contour colour coding shown on top. Velocity vectors delineate a circular area for which the circulation around the peak vorticity is maximised and within which the vortex strength was computed by a surface quadrature. (*f*) Vortex strength along the wake. (*g*) Inflow velocity oscillation upstream of the cylinder. (*h*) Cross-flow oscillation of the wake at the location of maximum intensity $\{x/D, y/D\} = \{1.2, 0\}$.

A feature that stands out in figure 2(*f*) is the sudden drop in vortex strength. Whether this feature is real or artificial is debatable. A possible physical mechanism is the cross-annihilation of oppositely signed vorticity in the near wake due the flapping motion of the shear layer. The negative vortex appears to be attached to the

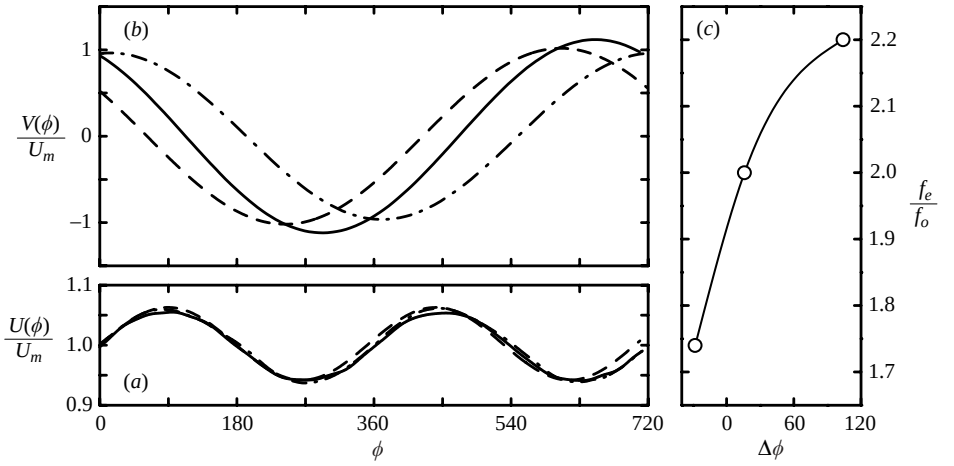

FIGURE 3. (*a*) Inflow velocity oscillation; (*b*) cross-flow oscillation of the wake; (*c*) phase-difference between $U(\phi)$ and $V(\phi)$. – – $f_e/f_o = 1.74$; — $f_e/f_o = 2.00$; – · – $f_e/f_o = 2.20$.

cylinder by a strand of vorticity extending all the way to its generator in figure 2(*a–d*). A careful look at the velocity vectors in figure 2(*b*) shows that the vectors within the strand of vorticity connection are nearly normal to the tangent of the circle delineated by the vectors at this particular phase. It might be argued that the vortex is no longer fed with circulation from the cylinder and is, thus, shed. The sharp decrease in vortex strength coincides with the occurrence of the maximum cross-flow oscillation, i.e. $V(\phi) = V_{\max}$, which is caused by the entrainment of the shear layer across the wake axis cutting off the supply of vorticity and eventually determining the timing of vortex shedding. The same feature was observed at other perturbation frequencies for which the wake exhibits a slightly different morphology as is shown further below.

According to the analysis presented above, it is deemed appropriate to use the relative phase between $U(\phi)$ and $V(\phi)$ in order to examine the variation in the timing of vortex shedding as f_e/f_o is varied across the synchronization range (2S mode). Figure 3 shows the response of the $V(\phi)$ oscillation across the wake axis to the imposed inflow perturbation $U(\phi)$ at the three different frequencies. All lines shown are sine fits to the actual velocity data; $U(\phi) = U_m + \Delta U \sin(\phi)$ curves are based on phase-averaged LDV data obtained upstream of the test cylinder; $V(\phi) = V_{max} \sin(\phi/2 + \Delta\phi)$ curves are based on phase-averaged DPIV data obtained in the wake and correspond to the location of maximum cross-flow oscillation along the wake axis; $x/D = 1.2$, 1.2 and 1.3 at $f_e/f_o = 1.74$, 2.00 and 2.20, respectively. It should be noted that the sign of $V(\phi)$ determines whether a vortex is shed from the upper or the lower side once per oscillation and that the flow field is a mirror image with respect to the wake axis for a phase-shift of 360°. As f_e/f_o is varied there is a gradual change in the phase of $V(\phi)$ with respect to the phase of $U(\phi)$. At $f_e/f_o = 1.74$, $V(\phi)$ leads $U(\phi)$ by $\Delta\phi = -28°$ whereas the opposite occurs at $f_e/f_o = 2.20$ ($\Delta\phi = 104°$). As discussed above, the timing of vortex shedding occurs near the phase of $V(\phi) = V_{\max}$. This implies that a vortex is shed in each forward stroke of the oscillating cylinder within the synchronization range which corresponds to phase-angles between $\phi = 180°$ and 360°. The implications of this assertion for the in-line free vibration response of a flexibly mounted circular cylinder will be discussed in § 4. When the imposed wake frequency is lower than the natural one, the period of vortex shedding is

increased compared to the natural. The wake responds to this effect by shifting the timing of vortex shedding to occur earlier in the cycle and at the beginning of the forward stroke, e.g. $V_{\max} = V(244^\circ)$ at $f_e/f_o = 1.74$. This is like trying to adhere to a universal formation process (Jeon & Gharib 2004). The inverse occurs at frequencies greater than the natural wake frequency; the wake adjusts the timing of vortex shedding to occur later in the cycle and towards the end of the forward stroke. In fact, $V_{\max} = V(376^\circ)$ at $f_e/f_o = 2.2$ which corresponds to the beginning of the backward stroke (see § 4). At the middle of the lock-on range, i.e. $f_e/f_o = 2$, the perturbations interact with the natural vortex formation process which brings about a remarkable intensification of the wake fluctuations and the fluid forces exerted on the cylinder as has been consistently observed in previous related studies (Tanida, Okajima & Watanabe 1973; Barbi *et al.* 1986, Armstrong, Barnes & Grant 1987; Konstantinidis *et al.* 2003).

Figure 4 shows the phase-referenced vorticity distributions in the wake at the three perturbation frequencies employed. The phase shown in each case was selected to give the best possible match among the different frequencies based on the $\Delta\phi$ estimates found above. A close correspondence of the wake patterns can be observed. The vorticity contours show a positive (rotating counter-clockwise) vortex on the lower side at the timing of shedding, even though the vortex appears connected to the cylinder by a vorticity strand. Upon examining the vorticity distributions in figure 4, the fact that the longitudinal spacing between the vortices varies inversely proportionally with the frequency ratio f_e/f_o should be taken into account (Griffin & Ramberg 1976; Konstantinidis *et al.* 2003). As a result of this effect, the wake pattern appears expanded and contracted for frequencies below and above, respectively, the natural wake frequency. This effect should not be confused with the variation of the vortex formation region. If the formation length l_f is defined as the location along the wake axis where the streamwise velocity fluctuation becomes strongest, then $l_f/D = 1.0$, 1.1 and 1.3 at $f_e/f_o = 1.74$, 2.00 and 2.20, respectively (cf. to the value of 2.3 in unforced flow). Previous detailed LDV measurements along the wake axis have clearly shown that the formation length is minimized in the middle of the lock-on range (Konstantinidis *et al.* 2003). It should be noted that the perturbation frequency has a remarkable effect on the morphology of the shed vortex. Referring to the positive vortex on the lower side of the cylinder, a gradual modification from a rather circular shape at $f_e/f_o = 1.74$ to an elliptical one with its minor axis nearly aligned with the flow at $f_e/f_o = 2.20$ is observed. This feature demonstrates the complexity of the fluid mechanics and of the interaction between the natural wake instability and the imposed perturbation. Even these subtle differences in the vorticity distribution can have a pronounced effect on the fluid forces imparted to the cylinder as shown by related force measurements (Tanida *et al.* 1973; Nishihara, Kaneko & Watanabe 2005).

4. Discussion

The response of a flexibly mounted circular cylinder to vortex-induced vibration depends on a number of flow and structural parameters, see e.g. Bearman (1984) for a review on the subject. Given the structural parameters, the amplitude of vibration can be described in terms of a main parameter: the reduced velocity $U^* = U_m/f_n D$ where f_n is the natural vibration frequency of the structure. On the other hand, in forced oscillation studies the frequency and amplitude of oscillation, usually encountered in terms of the dimensionless parameters f_e/f_o and A/D, can

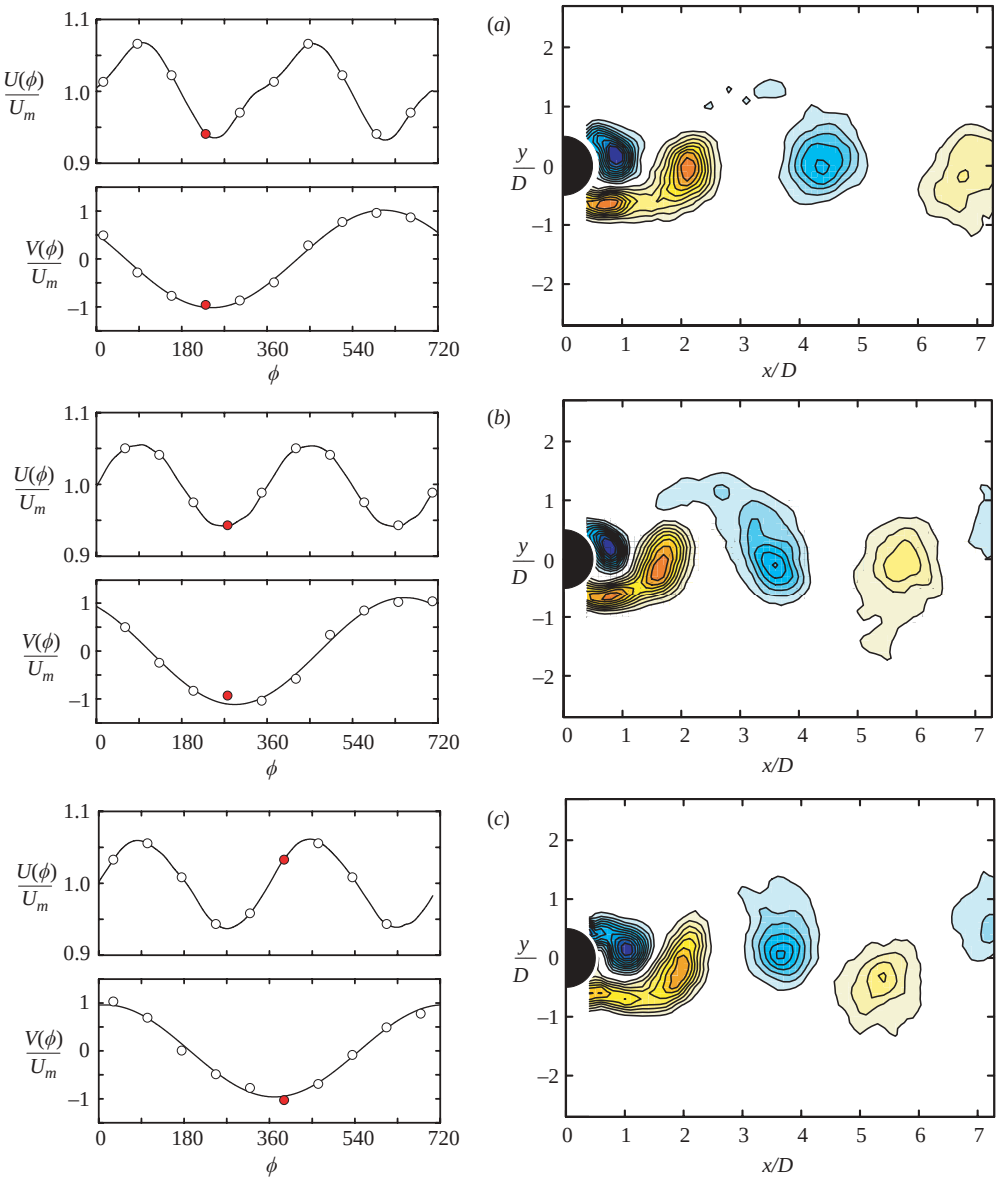

FIGURE 4. Phase-averaged vorticity distribution in the forced wake at the phase that a positive vortex is shed from the lower side of the cylinder together with the corresponding points (red symbols) in the inflow and cross-flow oscillation. (*a*) $f_e/f_o = 1.74$; (*b*) $f_e/f_o = 2.00$; (*c*) $f_e/f_o = 2.20$. Contour colour coding as in figure 2.

be varied independently. Correlating free and forced cylinder studies may be viewed as a transformation of the independent variables $f_e \leftrightarrow f_n$. The structural frequency f_n acts as an excitation frequency in free vibrations. This transformation appears straightforward but one needs to be careful because the frequency at which the cylinder responds can be different from f_n, depending on the combined flow and structural parameters (Williamson & Govardhan 2004). In practice, however, the cylinder vibration and the wake synchronize at a frequency sufficiently close to f_n.

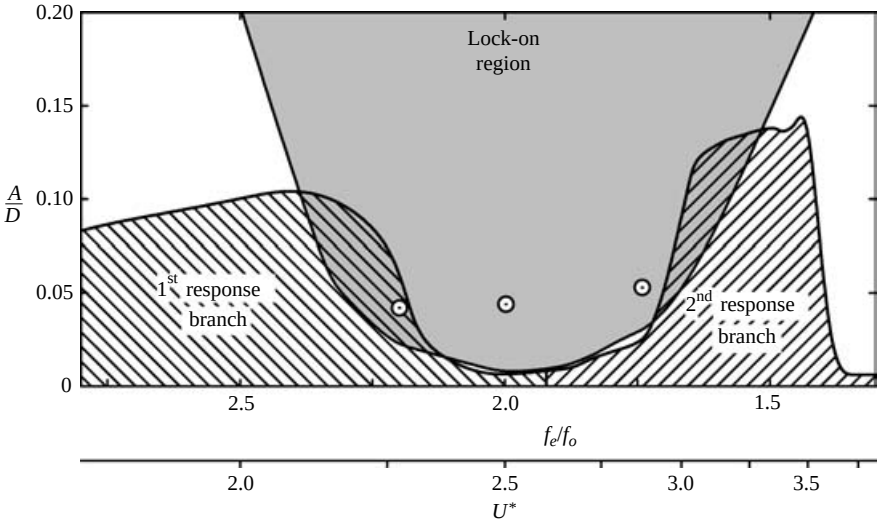

FIGURE 5. The lock-on region found in forced cylinder oscillations in-line with the flow juxtaposed with the response branches of a flexibly mounted cylinder free to vibrate in-line with the flow. Lock-on envelope produced from the data in Konstantinidis *et al.* (2003). Positive excitation envelope reproduced from published data in Okajima *et al.* (2004). Bull's eye symbols indicate the present experimental data.

A flexibly mounted cylinder restrained to vibrate only in-line with the flow direction exhibits two positive excitation regions, or response branches, as U^* is varied. Paradoxically, these two branches lie on either side of the lock-on region found in forced oscillation studies, which occurs around $U^* \approx 1/2S \approx 2.5$. This is illustrated in figure 5 where the lock-on region for forced oscillations and the positive excitation regions for free vibrations in-line with the flow are juxtaposed. The transformation $f_e \leftrightarrow f_n$ has been employed so that $U^* = S^{-1}(f_e/f_o)^{-1}$. When $U^* < 1/2S$, symmetric vortex formation on both sides of the cylinder occurs while for $U^* > 1/2S$ the antisymmetric 2S vortex pattern is observed (Naudascher 1987; Okajima *et al.* 2004). It should be noted that the response depends on the combined flow and structural parameters. The positive excitation regions shown are after the recent measurements of Okajima *et al.* with the lowest combined mass damping. In this condition the highest amplitude response was observed so that the hatched area in figure 5 encompasses all the measured response curves.

The behaviour observed in figure 5 implies that over the lock-on range in which the forces acting on a forcibly oscillating cylinder are magnified (Tanida *et al.* 1973; Barbi *et al.* 1986; Nishihara *et al.* 2005), the in-line response of a freely vibrating cylinder is negligible. This seemingly paradoxical behaviour may be explained by extending the concept of the vortex lift force to the drag direction (Carberry *et al.* 2004). The fluctuating drag force may be regarded as the sum of two components: an apparent mass force due to the displaced fluid and a vortex drag force due to the vorticity distribution in the wake. Since the apparent mass force is always in-phase with the relative cylinder motion, the phase of the total drag force is determined by the phase of the vortex force, i.e. by the vorticity distribution in the wake relative to the cylinder motion. The lack of cylinder excitation inside the lock-on range, i.e. $f_e/f_o \approx 2$, implies that the vortex drag force opposes the cylinder motion (damping force). Interestingly, measurements of the phase of the total drag force predict this

behaviour correctly; the out-of-phase component of the drag force is negative near the middle of the lock-on range (Tanida *et al.* 1973; Nishihara *et al.* 2005). Similarly, when the cylinder is free to vibrate, the vortex drag force does not excite vibrations for frequencies in the lock-on range. The present study links this behaviour to the timing of a shedding vortex during the forward stroke of the cylinder that induces a negative excitation from the fluid.

As discussed in § 3, the timing of vortex shedding is gradually shifted towards the backward stroke of the cylinder as the reduced velocity increases or decreases from $U^* \approx 2.5$ ($f_e/f_o \approx 2$). This enables a positive coupling between the vortex force and the cylinder motion to be established as the frequency limits of the lock-on range are approached and, therefore, vortex-induced vibrations ensue. Although the present analysis correctly suggests a positive coupling at $f_e/f_o = 2.2$ which is inside the first response branch in figure 5, it should be noted that the wake pattern observed in the present forced-oscillation study corresponds to antisymmetric vortex shedding (2S mode), whereas the first excitation region is associated with symmetric vortex shedding. Naudascher (1987) classified the latter as motion-induced excitation or 'wake-breathing'. This is a remarkable feature that highlights the intrinsic differences between forced and free vibrations. The self-excited vibration of flexibly mounted cylinders in the two excitation regions and the corresponding wake patterns is beyond the scope of the present study but it is hoped that the discussion presented will improve understanding of this problem and stimulate further the research interest in it. It seems plausible that a phase 'jump' or transition might exist near the end of the first response branch to account for the change in the wake pattern. Furthermore, the overlap between the lock-on and positive excitation regions on either side might indicate hysteresis effects.

Finally, it is intriguing to ask if inflow perturbations may be used to damp the free vibrations of flexibly mounted rigid cylinders or even those of flexible cylinders. Based on the discussion presented above, it is conjectured that periodic inflow perturbations or any means that can control the timing of vortex shedding in the cylinder wake may, in principle at least, be used to suppress the free vibrations. This approach departs from the established methodologies used for the reduction of vortex-induced vibrations of cylindrical structures which have focused on the destruction of vortex shedding, e.g. by three-dimensional geometric perturbations.

Partial support for conducting this research was provided by the Engineering and Physical Sciences Research Council U.K. under grant GR/R29802/01.

REFERENCES

Armstrong, B. J., Barnes, F. H. & Grant, I. 1987 A comparison of the structure of the wake behind a circular cylinder in steady flow with that in a perturbed flow. *Phys. Fluids* **30**, 19–26.

Barbi, C., Favier, D. P., Maresca, C. A. & Telionis, D. P. 1986 Vortex shedding and lock-on of a circular cylinder in oscillatory flow. *J. Fluid Mech.* **170**, 527–544.

Bearman, P. W. 1984 Vortex shedding from oscillating bluff bodies. *Annu. Rev. Fluid Mech.* **16**, 195–222.

Cantwell, B. & Coles, D. 1983 An experimental study of entrainment and transport in the turbulent near wake of a circular cylinder. *J. Fluid Mech.* **136**, 321–374.

Carberry, J., Govardhan, R., Sheridan, J., Rockwell, D. & Williamson, C. 2004 Wake states and response branches of forced and freely oscillating cylinders. *Eur. J. Mech.* B *Fluids* **23**, 89–97.

Gerrard, J. H. 1966 The mechanics of the formation region of the vortices behind bluff bodies. *J. Fluid Mech.* **25**, 401–413.

Griffin, O. M. & Ramberg, S. E. 1976 Vortex shedding from a cylinder vibrating in line with an incident uniform flow. *J. Fluid Mech.* **75**, 526–537.

Jeon, D. & Gharib, M. 2004 On the relationship between the vortex formation process and cylinder wake vortex patterns. *J. Fluid Mech.* **519**, 161–181.

Konstantinidis, E., Balabani, S. & Yianneskis, M. 2003 The effect of flow perturbations on the near wake characteristics of a circular cylinder. *J. Fluid Struct.* **18**, 367–386.

Konstantinidis, E., Balabani, S. & Yianneskis, M. 2004 A PIV study of the wake of a circular cylinder subjected to low amplitude flow perturbations. In *Proc. 8th Intl Conf. on Flow Induced Vibration* (ed. de Langre & Axisa). Ecole Polytechnique, Paris.

Konstantinidis, E., Balabani, S. & Yianneskis, M. 2005 Conditional averaging of PIV plane wake data using a cross-correlation approach. *Exps. Fluids* **39**, 38–47.

Naudascher, E. 1987 Flow-induced streamwise vibrations of structures. *J. Fluids Struct.* **1**, 265–298.

Nishihara, T., Kaneko, S. & Watanabe, T. 2005 Characteristics of fluid dynamic forces acting on a circular cylinder oscillated in the streamwise direction and its wake patterns. *J. Fluids Struct.* **20**, 505–518.

Okajima, A., Nakamura, A., Kosugi, T., Uchida, H. & Tamaki, R. 2004 Flow-induced in-line oscillation of a circular cylinder. *Eur. J. Mech.* B *Fluids* **23**, 115–125.

Ongoren, A. & Rockwell, D. 1988 Flow structure from an oscillating cylinder. Part 2. Mode competition in the near wake. *J. Fluid Mech.* **191**, 225–245.

Tanida, Y., Okajima, A. & Watanabe, Y. 1973 Stability of a circular cylinder oscillating in uniform flow or in a wake. *J. Fluid Mech.* **61**, 769–784.

Williamson, C. H. K. & Govardhan, R. 2004 Vortex-induced vibrations. *Annu. Rev. Fluid Mech.* **36**, 413–455.

Williamson, C. H. K. & Roshko, A. 1988 Vortex formation in the wake of an oscillating cylinder. *J. Fluids Struct.* **2**, 355–381.